



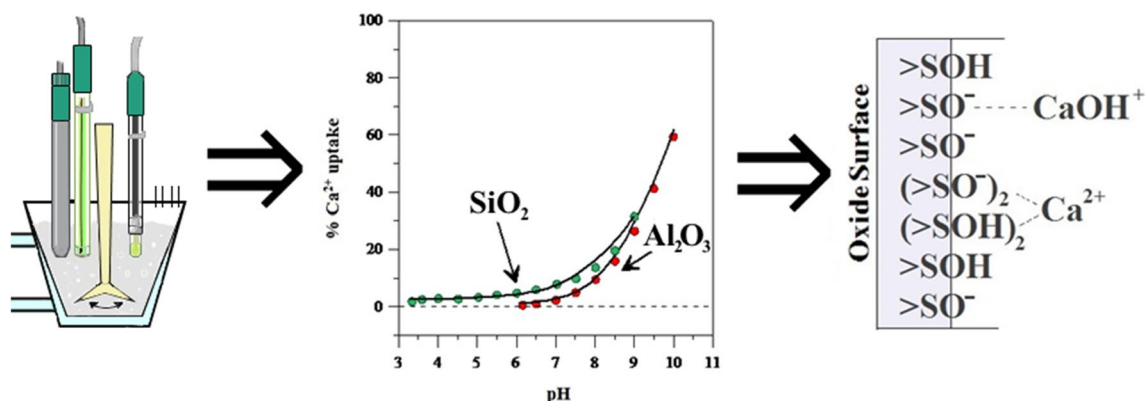
# Investigations of mechanism of $\text{Ca}^{2+}$ adsorption on silica and alumina based on Ca-ISE monitoring, potentiometric titration, electrokinetic measurements and surface complexation modeling

Karolina Szymanek<sup>1</sup> · Robert Charmas<sup>2</sup> · Wojciech Piasecki<sup>3</sup>

Received: 10 June 2020 / Revised: 17 October 2020 / Accepted: 27 October 2020 / Published online: 5 November 2020  
© The Author(s) 2020

## Abstract

Research on  $\text{Ca}^{2+}$  adsorption onto the mineral surface is of significant importance with regard to geochemical processes. Sverjensky (Geochim Cosmochim Acta 70(10), 2427–2453, 2006) assumed that alkaline earths form two types of surface species on oxides: tetranuclear  $(>\text{SOH})_2(>\text{SO}^-)_2\text{M}(\text{OH})^+$  and mononuclear  $>\text{SO}^-\text{M}(\text{OH})^+$ . To look into the above assumption we investigated calcium adsorption on  $\text{SiO}_2$  and  $\text{Al}_2\text{O}_3$  because they are the most widespread minerals in the environment. We have determined the proton surface charge, electrokinetic potential and metal adsorption as a function of pH. The  $\text{Ca}^{2+}$  uptake and concentration in the system were monitored by the calcium ion-selective electrode (Ca-ISE). The Ca-ISE measurements indicated a similar affinity of  $\text{Ca}^{2+}$  for both materials despite their differently charged surface, negative for silica and mainly positive for alumina. This may suggest that simple electrostatic interactions are not the primary driving force for calcium adsorption, and that solvation of calcium ions at the surface may be crucial. We have analyzed our experimental data using the 2-pK triple-layer model (2-pK TLM). Three calcium complexes on the mineral surface were reported. Two of them were the same for both oxides, i.e. the tetranuclear  $(>\text{SOH})_2(>\text{SO}^-)_2\text{Ca}^{2+}$  and mononuclear complexes  $>\text{SO}^-\text{CaOH}^+$ . Additionally, minor contribution from  $>\text{SOH}\dots\text{Ca}^{2+}$  for silica was assumed. In the case of  $\text{Al}_2\text{O}_3$  the hydrolyzed tetranuclear complexes  $(>\text{SOH})_2(>\text{SO}^-)_2\text{CaOH}^+$  at  $\text{pH} > 7.5$  occurred based on the modeling results. Two types of surface complexes suggested by Sverjensky allowed for the correct description of proton and calcium uptake for alumina. However, the electrokinetic data excluded hydrolyzed tetranuclear surface species for this oxide.



**Keywords** Calcium ion  $\text{Ca}^{2+}$  · Ion adsorption · Modeling · Silica  $\text{SiO}_2$  · Alumina  $\text{Al}_2\text{O}_3$  · Calcium ion-selective electrode Ca-ISE · Electrokinetic potential

✉ Karolina Szymanek  
karolina.szymanek@awf-bp.edu.pl

Extended author information available on the last page of the article

## 1 Introduction

In the soil and water environment calcium ions are of great importance (Stumm and Morgan 1996). They are crucial for the functioning of living organisms, the stability of natural systems and soil fertility (Wuddivira and Camps-Roach 2006; Clapham 2007; Eijssink et al. 2011; McGrath et al. 2014). Therefore, calcium has been commonly investigated, among others, with regard to adsorption on different metal oxides. It was shown that the latter process evidently depends on many factors, for instance, pH, temperature, ionic strength, and the presence of organic matter (Atesok et al. 1988; Ridley et al. 1999; Weng et al. 2008; Lee et al. 2014; Allen et al. 2017; Cherian et al. 2018; Jia et al. 2019).

Minerals such as silica and alumina constitute particles widely spread in the Earth's crust (Sparks 2003). From the point of view of  $\text{SiO}_2$  application, it is an efficient sealant, food additive, adsorbent and common filler for drugs and cosmetic powders and can be also applied as clinical materials (Barbé et al. 2004; Regi-Vallet and Balas 2008; Bui and Choi 2010; Fruijtier-Pölloth 2016; Floch et al. 2018; McCarthy et al. 2018; Steiling et al. 2018). Aluminum(III) oxide is useful in terms of catalysis, adsorption, pigmentation of paints and cosmetics as well as constituting electronic devices (Cheah et al. 1998; Teaney et al. 1999; Kasprzyk-Hordern 2004; Chasserio et al. 2009). The particles of both oxides remaining in water are in a continuous contact with  $\text{Ca}^{2+}$  in the soil environment. Remembering that assemblages of these oxides from the industry sector are still released into the natural system (Kasprzyk-Hordern 2004; Lee et al. 2010), research on their behavior towards calcium ions was carried out over the past decades (Roach and Himmelblau 1961; Huang and Stumm 1973; Meng and Letterman 1993; Brigante and Avena 2016; Ragab et al. 2017; Wan et al. 2019). For example, Tadros and Lyklema (1969) investigated calcium adsorption on silica using potentiometric titrations and the Eppendorf flame photometer. They concluded that physical sorption of  $\text{Ca}^{2+}$  on the silica surface appeared at pH below 7.5. Above this pH region specific adsorption occurred. Meng and Letterman (1993) characterized silica via the deuterium exchange, TEM, electrokinetic measurements and performed adsorption experiments using the atomic absorption spectrophotometer. Lützenkirchen and Behra (1997) modeled the latter experimental data using the modified FITEQL program (Westall 1982). A different method of calcium determination in the silica dispersion was used by Janusz et al. (2003), i.e. the radiotracer technique. Those investigations showed that the higher  $\text{NaClO}_4$  electrolyte concentration, the lower  $\text{Ca}^{2+}$  adsorption occurred confirming the earlier findings by

Kosmulski (1994) who used the same technique for both alumina and silica in NaCl solution. Previously, the distribution of the alkaline earth ions at the alumina–electrolyte interface was estimated using alkalimetric and acidimetric titration curves (Huang and Stumm 1973). The most recent research discussed divalent (among others  $\text{Ca}^{2+}$ ) and monovalent adsorption affinity for the  $\alpha\text{-Al}_2\text{O}_3$ /water interface using the vibrational sum frequency generation (vSFG) (Piontek et al. 2019).

Besides the studies cited above, there does not seem to be any report about research on calcium adsorption in the above mineral systems in particles sizes in the range of nanometers applying the calcium ion-selective electrode (Ca-ISE). Therefore, in this study an attempt was made to characterize the mineral/water interface concerning the  $\text{Ca}^{2+}$  adsorption on  $\text{SiO}_2$  and  $\text{Al}_2\text{O}_3$  in a wide pH range using the Ca-ISE. Applying Born solvation and crystal-chemical theory Sverjensky (2006) assumed that alkaline earths adsorbed on minerals forming tetranuclear  $(>\text{SOH})_2(>\text{SO}^-)_2\text{-M}(\text{OH})^+$  and mononuclear  $>\text{SO}^-\text{-M}(\text{OH})^+$  surface complexes. Our aim was to examine whether in our systems the same adsorption mechanism could be applied. For this purpose the methods applied in our recent paper (Szymanek et al. 2020), i.e. direct potentiometry for monitoring  $\text{Ca}^{2+}$  concentration,  $\zeta$ -potential measurements, and surface complexation 2-pK TLM (triple-layer model) with the GEOSURF program developed by Sahai and Sverjensky (1998) were used.

## 2 Experimental section

The materials that are the commercial hydrophilic fumed silica ( $\text{SiO}_2$ , AEROSIL 200, 99.8%) and alumina ( $\text{Al}_2\text{O}_3$ , AEROXIDE Alu C, 99.8%) were obtained from the Evonik Company. The detailed properties of these solids were provided by the manufacturer. The specific surface area (BET) of  $\text{SiO}_2$  was equal to  $200 \pm 25 \text{ m}^2 \text{ g}^{-1}$  and for  $\text{Al}_2\text{O}_3$  it was  $100 \pm 15 \text{ m}^2 \text{ g}^{-1}$ . Nanopowder of silica had an amorphous form and its average size of elementary particles was about 14 nm. The applied alumina nanoparticles were composed of  $\gamma$  (66%) and  $\delta$  (33%) structures of the particle size in the range of 7 to 20 nm. The raw materials were subjected to the experiment without further purification. The applied chemicals, the experimental setup and the conditions were the same as described in our previous paper (Szymanek et al. 2020).

The acid-base properties of  $10 \text{ g dm}^{-3}$  of oxides in the KCl solutions were determined using potentiometric titrations at three ionic strengths (0.1, 0.01, 0.001 M) starting from the acidic pH. The net proton consumption curves were also determined for the same samples in 0.1 M and 0.01 M KCl with 1 mM  $\text{Ca}^{2+}$  and also with 10 mM  $\text{Ca}^{2+}$  in the case of silica. This amount of calcium was compared

to that found in the surface waters. The surface charge  $\sigma_H$  was calculated in the way presented by Piasecki et al. (2019). Next, the samples were subjected to  $Ca^{2+}$  uptake experiments in which the concentration of free calcium ions was checked every 0.5 pH unit by Ca-ISE used also in our previous study (Prus et al. 2019) as well as applying the spectrophotometric method (Kendrick et al. 1977) as a reference. In a separate experiment the dependence of the electrokinetic potential ( $\zeta$ ) of the dispersions with and without 1 mM  $Ca^{2+}$  in 0.01 M KCl as a function of pH at 25 °C was determined using the Malvern Zetasizer Nano ZS equipped with the MPT-2 autotitrator and a high concentration zeta cell. The  $\zeta$ -potential was calculated from the electrophoretic mobility using the Smoluchowski equation (Pashley and Karaman 2004). Diluted samples and lower ionic strength were tested to ensure optimal particle mobility (1 g dm<sup>-3</sup> of oxide in the 0.01 M KCl) (Delgado et al. 2005). The results obtained from the Medusa speciation program (Puigdomenech 2001) indicate that in the studied system  $CaCl^+$  ions are present at a constant concentration of about  $2 \times 10^{-5}$  M, and the concentration of  $CaOH^+$  ions is negligible.

In this study theoretical investigations were carried out using the 2-pK TLM modeling approach (Yates et al. 1974; Davis et al. 1978; Sverjensky 2005, 2006) in accordance with our recent paper (Szymanek et al. 2020).

### 3 Results and discussion

#### 3.1 Net proton consumption

The examined oxides exhibited quite different behavior in terms of the proton consumption function in KCl solutions (Fig. 1). The precise location of the silica PZC could not be observed since the proton surface charge density curves did not intersect at one exact point, but remained superimposed (a plateau was observed at pH 3–5). Previous literature provided many varying assumptions of PZC value from titrations in the case of silicon dioxide showing the difficulties in its determination (Tadros and Lyklema 1969; Sahai 2002; Milonjić et al. 2007; Kosmulski 2009).

One could observe that the surface of SiO<sub>2</sub> was negatively charged nearly in the whole studied pH range starting with about 3 up to 9. Silica may dissolve at alkaline pH (Eikenberg 1990) and in our case at pH > 9 this could lead to a large base consumption. Hence there was no point in performing titration in that pH region. In the case of Al<sub>2</sub>O<sub>3</sub> the determined PZC corresponding to the common intersection point of the charge curves was about 8.8 consistent with the values in the range 8.4–9.4 reported in the literature (Huang and Stumm 1973; Regalbuto et al. 1999; Szekeres and Tombácz 2012). Contrary to silica, the alumina surface was positively charged under most measured pH conditions. According to the paper by Tombácz and

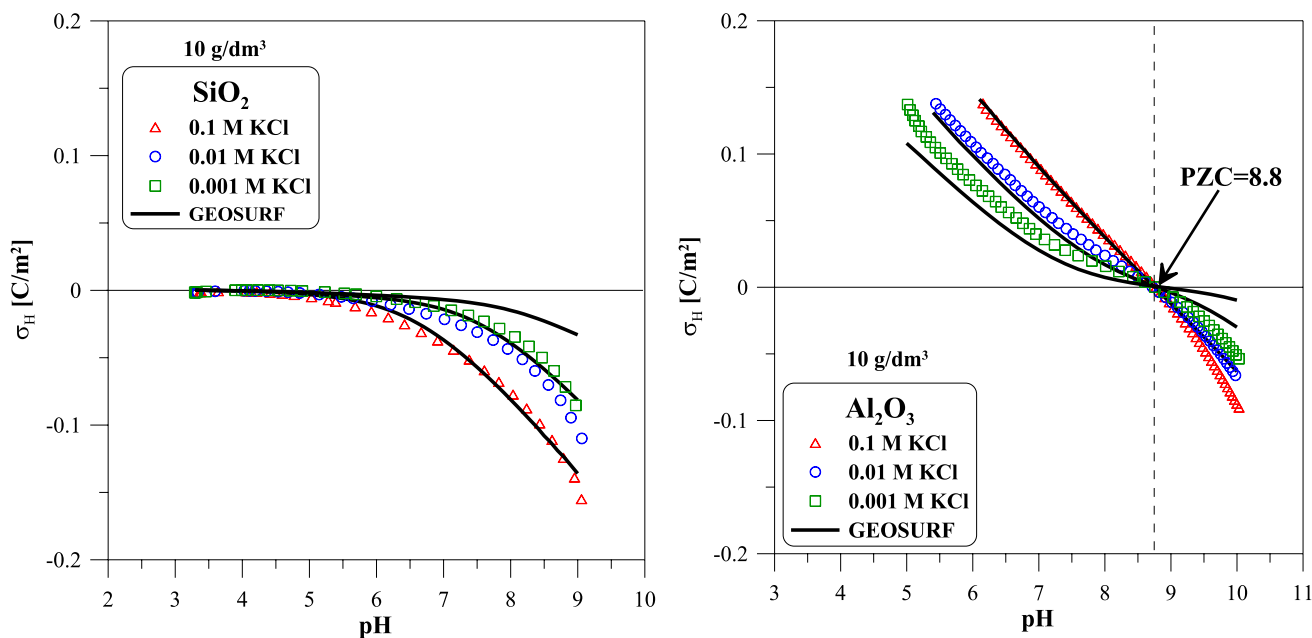


**Fig. 1** The pH dependence of the proton surface charge density  $\sigma_H$  (C/m<sup>2</sup>) of SiO<sub>2</sub> and Al<sub>2</sub>O<sub>3</sub> in the 0.1 M (red triangles), 0.01 M (blue circles), and 0.001 M KCl (green squares) likened with the GEOSURF model fitting (continuous line) for the oxide concentra-

tion of 10 g dm<sup>-3</sup>. The PZC corresponding to the common intersection point of charge curves (CIP) was not clearly defined for SiO<sub>2</sub> (PZC=3–4) and for Al<sub>2</sub>O<sub>3</sub> it was equal to 8.8 (Color figure online)

Szekeres (2001) in this type of measurements,  $\text{Al}_2\text{O}_3$  particles can undergo dissolution at low ( $\text{pH} < 4.5$ ) and at high pH ( $\text{pH} > 9.5$ ) which is shown here by the steepness of the proton surface charge curves. In order to avoid dissolution in acidic region, titrations were performed from  $\text{pH} > 5$ . Due to the formation of  $\text{Al}(\text{OH})_4^-$  species, the consumption of hydroxide ions may take place.

The theoretical calculations fitted sufficiently the experimental data for both oxides at 0.1 and 0.01 M ionic strengths. The most visible discrepancy was noted at the lowest ionic strength (0.001 M KCl), possibly as a result of the change in ionic strength during titration. To keep a constant value of PZC we assumed symmetric constants for adsorption of electrolyte ions (i.e. cation and anion have the same affinity for the surface). However, using symmetric constants it was difficult to obtain a good fit to the asymmetric experimental data. Nonetheless, this was not of much significance for our experiment on calcium adsorption conducted for 10 g  $\text{dm}^{-3}$  of oxides at 0.1 M ionic strength. Modeling for silica was presented previously in several articles (Sahai and Sverjensky 1997; Atalay et al. 2014) in which the trend of the proton surface charge density curves partially corresponded to ours. The assumed capacitance  $c_1$  in 2-pK TLM for  $\text{SiO}_2$  was about  $1.3 \text{ F m}^{-2}$ , similar to that found by Sverjensky (2005), and the  $c_2$  value of  $0.1 \text{ F m}^{-2}$  was smaller than that commonly applied in other papers, i.e.  $0.2 \text{ F m}^{-2}$  (Sahai and Sverjensky 1997; Villalobos and Leckie 2001; Sverjensky 2005), but inevitable in order to obtain well fit in the case of the  $\zeta$ -potential data shown in the further part of this study (Fig. 5). As regards  $\text{Al}_2\text{O}_3$ , the value for both capacitances was equal to  $1.2 \text{ F m}^{-2}$ . Similar values of  $c_1$  were also used previously (Davis et al. 1978; Toner and Sparks 1995; Tombácz and Szekeres 2001). On the negatively charged surface of the alumina (above PZC) at the ionic strengths 0.01 and 0.001 M the model did not work properly demonstrating higher values of the proton surface charge.

The next experiment provided an interesting insight into the influence of calcium on the proton surface charge density  $\sigma_{\text{H}}$  for both oxides as a function of pH (Fig. 2). First of all, it demonstrated that the presence of calcium in the dispersion of silica did not change the net proton charge in a significant way at higher ionic strength (Fig. 2, top left panel). An increase in the calcium concentration led to evident extra release of  $\text{H}^+$  from the silica surface. Moreover, the pronounced  $\text{H}^+$  release was attributed to the decrease of the proton surface charge density caused by  $\text{Ca}^{2+}$  sorption in the 0.01 M KCl (Fig. 2, bottom left panel). The separation of the charge curves started at  $\text{pH} > 6$ . Comparing the proton surface charging of silica at two ionic strengths and two different concentrations of calcium ions it can be concluded that  $\text{K}^+$  and  $\text{Ca}^{2+}$  compete for the silica surface.

In the case of alumina (Fig. 2, top right panel) the calcium influence became evident above pH about 8 independently

of the ionic strength. In this range the value of the net proton surface charge decreased more significantly due to the  $\text{H}^+$  release into the dispersion medium compared with that of silica. This indicates the onset of  $\text{Ca}^{2+}$  adsorption onto the positively charged alumina surface. Moreover, one could observe that at the lower ionic strength at  $\text{pH} > 9$  the model did not fit the data from titration. This may result from the troubles with the electrode readings, among others, due to the dissolving effect of the oxide. Among others, a relevant change of the ionic strength was possible there. Also at lower ionic strength in the high pH range the net proton charge for the system of  $\text{Al}_2\text{O}_3$  with  $\text{Ca}^{2+}$  revealed the most negative value ( $-0.226 \text{ C m}^{-2}$  at pH 10), which confirms possible dissolution of aluminum oxide particles at this pH value.

### 3.2 $\text{Ca}^{2+}$ uptake experiment

The  $\text{Ca}^{2+}$  uptake data as a function of pH in the oxide dispersions in the form of adsorption edges are presented compared with the modeling in Fig. 3. The results from both CaISE and spectrophotometry were consistent. Surprisingly, the trend of the adsorption edges of both oxides revealed a similarity. One could observe a comparable amount of adsorbed  $\text{Ca}^{2+}$  (about 30%) at pH 9 for both silica and alumina. Despite the oppositely charged surface of oxides (except for  $\text{pH} \geq 9$ ), they exhibit a similar affinity for calcium ions. In the case of silica small  $\text{Ca}^{2+}$  uptake (less than 5%) at pH ranging from 3 to 6 was reported. Above this pH range the adsorption started to increase more significantly. Janusz et al. (2003) observed almost the same amount of calcium adsorption as in our case at pH from 6 to 9 even using a different technique. However, unlike us, he demonstrated zero level  $\text{Ca}^{2+}$  uptake at pH up to 6. Although Kosmulski (1994) investigated silica at a different temperature from ours and washed minerals with nitric acid, and then with water, his results are analogous at pH from 4 to 8. The negatively charged silica surface showed weak binding of the calcium ions contrary to the expectations related to their strong Coulombic attraction. This can be explained by the impeding  $\text{Ca}^{2+}$  adsorption due to the tighter hydration shell of some sorption sites than that of adsorbate (steric hindrance for the ion hydration shells) (Döpke et al. 2019).

As regards alumina, calcium ion adsorption appeared at  $\text{pH} > 6$  and thus below its PZC, which is in agreement with the literature reports (Huang and Stumm 1973). Above pH 8, the adsorption edge was steeper showing stronger adsorption. This experiment corroborated findings of Piontek et al. (2019) that divalent and monovalent cations demonstrated a similar behavior towards  $\text{Al}_2\text{O}_3$  at low pH, however, at pH 10 the calcium ions predominated in terms of the adsorption affinity for the mineral surface. These authors also found that  $\text{Ca}^{2+}$  rearranges extensively the interfacial hydrogen

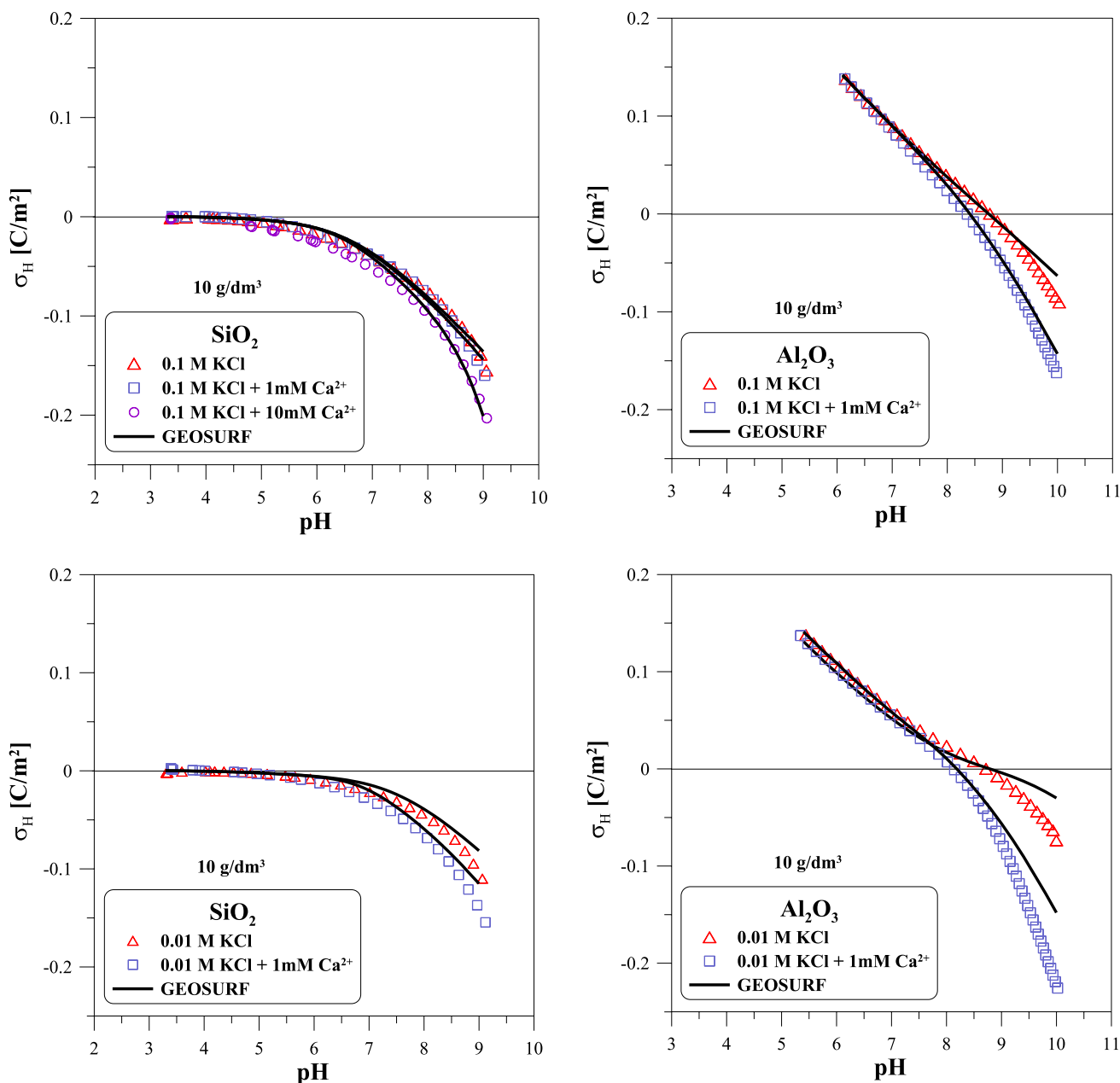


**Fig. 2** The pH dependence of the proton surface charge density  $\sigma_H$  (C/m<sup>2</sup>) of SiO<sub>2</sub> and Al<sub>2</sub>O<sub>3</sub> in the 0.1 M (top panel) and 0.01 M KCl (bottom panel) with 1 mM Ca<sup>2+</sup> (blue squares), 10 mM (vio-

let circles) and without (red triangles) likened with the GEOSURF model fitting (continuous line) for the oxide concentration of 10 g dm<sup>-3</sup> (Color figure online)

bonding environment near the negatively charged alumina surface which was practically not observed on the positively charged surface.

As results from the theoretical investigations properly fitted to the experimental data, calcium speciation shown in the right panels of Fig. 3 was obtained. Kosmulski (1994) suggested the reaction of simple monodentate species  $\equiv\text{SiO}-\text{Ca}^+$  formation on the silica surface, but that did not coincide with our findings. At the lower end of the pH range for the silica system, calcium would be

adsorbed only at the onset of the diffuse layer (DL) in the form of  $>\text{SOH}\dots\text{Ca}^{2+}$  which was assumed by Sverjensky (2006). At pH > 7 the tetranuclear complexes  $(>\text{SOH})_2(>\text{SO}^-)_2\text{Ca}^{2+}$  on the  $\beta$ -plane were formed and they predominated in the pH range 8–9 in which also the mono-species  $>\text{SO}^-\text{CaOH}^+$  appeared ( $\beta$ -plane). According to Sverjensky (2006) the hydrolyzed tetra-species  $(>\text{SOH})_2(>\text{SO}^-)_2\text{CaOH}^+$  were mostly responsible for the adsorption process. Again, this was not consistent with our observations considering modeling of the

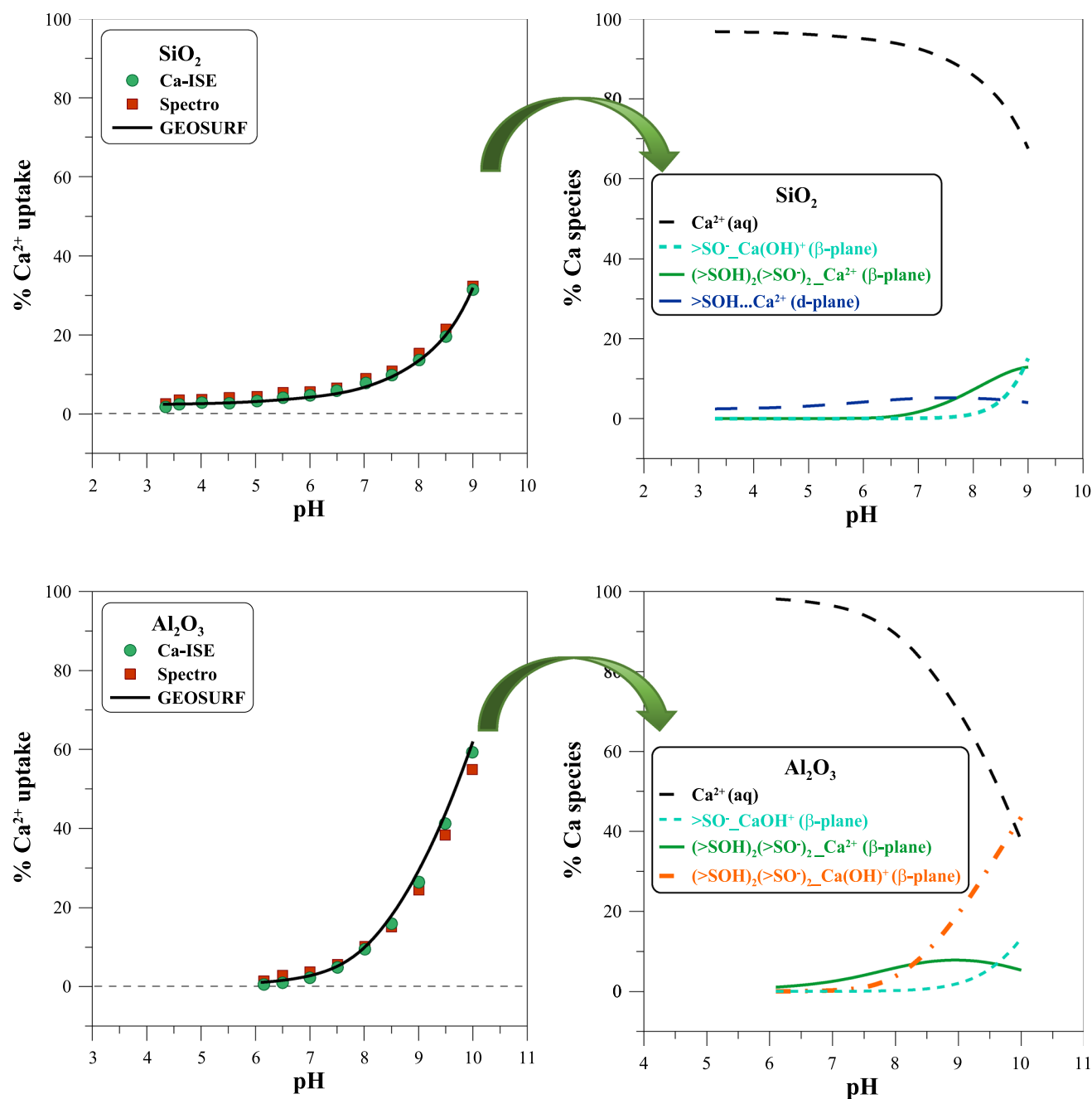


**Fig. 3**  $\text{Ca}^{2+}$  adsorption edges on  $\text{SiO}_2$  and  $\text{Al}_2\text{O}_3$  in the 0.1 M KCl + 1 mM  $\text{Ca}^{2+}$  determined by the Ca-ISE and spectrophotometric method likened with the GEOSURF model fitting (continuous line)

for the oxide concentration of  $10 \text{ g dm}^{-3}$ . The predicted calcium speciation as a function of pH (right panel) (Color figure online)

results from the electrokinetic measurements presented in Sect. 3.3 of this study. In the  $\text{Al}_2\text{O}_3$  system unhydrolyzed tetra-species, present also in the case of silica, were initially formed remaining at a low level (not exceeding 10%) till the end of the measurement. The hydrolyzed tetranuclear complexes  $(>\text{SOH})_2(>\text{SO}^-)_2\text{CaOH}^+$  were present at  $\text{pH} > 7.5$  and prevailed at pH of about 8.5 to 10. In addition, our calculations suggested minor occurrence

of mononuclear species  $>\text{SO}^- \text{CaOH}^+$  at  $\text{pH} > 9$ . All these complex structures appeared at the  $\beta$ -plane and they were in accordance with the assumptions by Sverjensky (2006) considering the tetranuclear complexes occurrence in the case of strontium ions based on the spectroscopic data from Fenter et al. (2000).

From the data fitting presented in Figs. 1, 2 and 3 the equilibrium constants (log K) shown in Table 1 were obtained.

The pH-dependence of surface coverage by Ca<sup>2+</sup> ions is presented in Fig. 4 for four oxides. The total number of the adsorption sites in millimoles in the adsorption system was calculated and it was equal for SiO<sub>2</sub> to 1.53 mmol, Al<sub>2</sub>O<sub>3</sub> 1.33 mmol, TiO<sub>2</sub> 1.04 mmol, Fe<sub>2</sub>O<sub>3</sub> 1.20 mmol. This confirms that the amount of calcium added into the experimental system (0.1 mmol) could be completely adsorbed by each of four oxide dispersions.

SiO<sub>2</sub> and Al<sub>2</sub>O<sub>3</sub> have similar and fairly low ability to adsorb Ca<sup>2+</sup> ions at pH up to 9 (Fig. 4) compared with the other oxides. In Fig. 4 one can notice that the surface coverage curves for silica and alumina almost overlap. It would seem that the negatively charged surface of silica strongly adsorbs Ca<sup>2+</sup> and thus an opposite effect can be expected for the positively charged alumina. This means that electrostatic interactions between the calcium ions and the surface of both oxides are not crucial for adsorption. Additionally, it follows from Fig. 2 that a high concentration of electrolyte weakens the interactions between Ca<sup>2+</sup> and the surface. For Fe<sub>2</sub>O<sub>3</sub> (maghemite) adsorption of Ca<sup>2+</sup> is slightly higher than for silica and alumina. Interestingly, maghemite and to a small extent silica are capable of Ca<sup>2+</sup> sorption even in the acidic range of pH (for Fe<sub>2</sub>O<sub>3</sub> below its PZC).

On the other hand, TiO<sub>2</sub> is the most efficient adsorbent for calcium ions. These observations suggest that there could be another factor than electrostatics which controls calcium adsorption on oxides. The Born solvation and crystal-chemical theory of ion adsorption on metal oxides enables explanation of these observations (Sverjensky 2005, 2006).

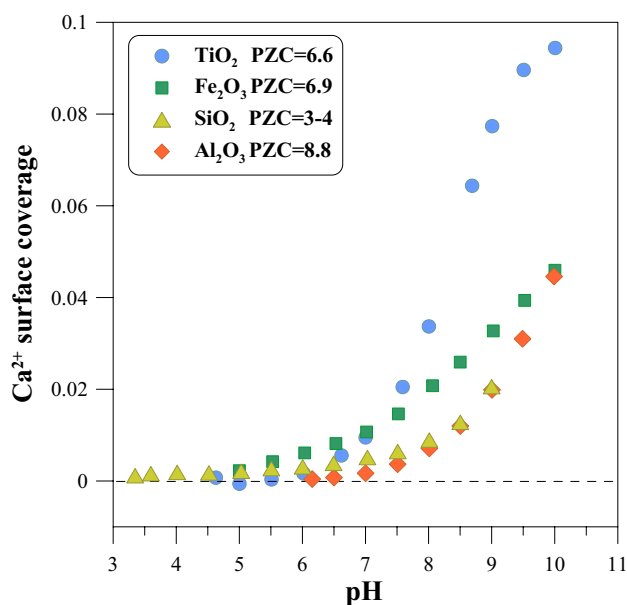


**Fig. 4** The pH-dependence of Ca<sup>2+</sup> surface coverage in the 0.1 M KCl+1 mM Ca<sup>2+</sup> for the oxide concentration of 10 g dm<sup>-3</sup>. The surface coverage was calculated by dividing the number of adsorbed calcium ions (in millimoles) by the total number of adsorption sites. The adsorption data for titania and maghemite are taken from the paper by Szymanek et al. (2020) (Color figure online)

Titanium dioxide has a very high dielectric constant (compared with those of silica and alumina) which indicates that the solvation contribution opposing adsorption disappears in this case.

Kosmulski (1994) noted that the adsorption of calcium on silica and alumina was independent of temperature. It means

**Table 1** The predicted equilibrium constants (log K) of the assumed surface reactions used in the GEOSURF program

Reaction	SiO <sub>2</sub> <sup>a</sup>	Al <sub>2</sub> O <sub>3</sub> <sup>b</sup>
	log K	log K
>SOH + H <sup>+</sup> → >SOH <sub>2</sub> <sup>+</sup>	- 0.1 <sup>c</sup>	6.1
>SOH → >SO <sup>-</sup> + H <sup>+</sup>	- 7.0	- 11.5
>SOH + K <sup>+</sup> → >SO <sup>-</sup> _K <sup>+</sup> + H <sup>+</sup>	- 6.8	- 9.2
>SOH + H <sup>+</sup> + Cl <sup>-</sup> → >SOH <sub>2</sub> <sup>+</sup> _Cl <sup>-</sup>	0.1 <sup>c</sup>	8.3
>SOH + Ca <sup>2+</sup> + H <sub>2</sub> O → >SO <sup>-</sup> _CaOH <sup>+</sup> + 2H <sup>+</sup> (mononuclear complex on β-plane)	- 14.5	- 16.8
4(>SOH) + Ca <sup>2+</sup> → (>SOH) <sub>2</sub> (>SO <sup>-</sup> ) <sub>2</sub> _Ca <sup>2+</sup> + 2H <sup>+</sup> (tetranuclear complex on β-plane)	- 7.0	- 10.0
4(>SOH) + Ca <sup>2+</sup> + H <sub>2</sub> O → (>SOH) <sub>2</sub> (>SO <sup>-</sup> ) <sub>2</sub> _Ca(OH) <sup>+</sup> + 3H <sup>+</sup> (tetranuclear complex on β-plane)	-	- 18.2
>SOH + Ca <sup>2+</sup> → >SOH...Ca <sup>2+</sup> (mononuclear complex on d-plane)	0.0	-

<sup>a</sup>SiO<sub>2</sub> properties: N<sub>s</sub> = 4.6 sites nm<sup>-2</sup>; c<sub>1</sub> = 1.3 F m<sup>-2</sup>, c<sub>2</sub> = 0.1 F m<sup>-2</sup>

<sup>b</sup>Al<sub>2</sub>O<sub>3</sub> properties: N<sub>s</sub> = 8 sites nm<sup>-2</sup>; c<sub>1</sub> = 1.2 F m<sup>-2</sup>, c<sub>2</sub> = 1.2 F m<sup>-2</sup>

<sup>c</sup>These parameter values for silica have no effect on the quality of the fit and have been chosen arbitrarily since the exact PZC value for this oxide is unknown

Where N<sub>s</sub> denotes the site density, c<sub>1</sub>, c<sub>2</sub> are the inner-layer and outer-layer capacitances in 2-pK TLM, respectively

>SOH represents the surface hydroxyl groups on the oxides

The equilibrium constants refer to the hypothetical 1.0 M standard state

that the enthalpy of this process is close to zero. It follows that calcium adsorption occurs as a result of an increase in entropy in the system during the accumulation of calcium ions at the surface. This confirms the importance of changes in solvation for the adsorption of these ions.

In the alkaline environment ( $\text{pH} > 9$ ) there is observed strong calcium binding to the oxide surface probably due to enhanced formation of hydrolyzed species  $\text{Ca}(\text{OH})^+$  at the surface.

As can be seen calcium adsorption depends on different factors influencing its magnitude and mechanism (e.g. ionic strength (Kosmulski 1994), the presence of other ions (Döpke et al. 2019)).

### 3.3 Electrokinetic potential

In order to study the adsorption phenomenon more profoundly, electrokinetic measurements were conducted. The experimental data are shown in Fig. 5 versus the modeling results. In the case of amorphous silica the negative value of the  $\zeta$ -potential was reported in the almost entire pH range of 3–9. The determined IEP for alumina was equal to the PZC value of 8.8 which was within the range of the previously investigated IEP values (Izrael Živković et al. 2015; Mayordomo et al. 2018; Ruchomski et al. 2018). Moreover, the results reported in the literature for silica (Kosmulski et al. 2002) and alumina (Izrael Živković et al. 2015) were quite consistent with the zeta potential curves obtained by us.

Comparing the results with and without calcium ions, raising of the  $\zeta$ -potential curves was found for both oxides due to the calcium adsorption. In the case of silica, a decrease in the zeta potential absolute value was observed. For alumina the electrokinetic potential became positive in the whole studied pH range. Moreover, the silica system with  $\text{Ca}^{2+}$  showed negative zeta potential values as presented also in the paper by Janusz et al. (2003). As regards  $\text{SiO}_2$  the curves from the electrokinetic measurements overlapped up to pH about 6 and then started to separate where the significant  $\text{Ca}^{2+}$  sorption occurred in compliance with the adsorption experiment (Fig. 3, left top panel) and with the net proton surface charge data (Fig. 2, left bottom panel). In the case of  $\text{Al}_2\text{O}_3$  the curve separation was observed at pH above 7.5 which also confirmed the beginning of the adsorption process presented in Sect. 3.2 as well as in the proton consumption curves (Fig. 2).

The model fitted the electrokinetic data excellently for the mineral systems without calcium. Furthermore, the validity of recalculation procedure proposed by Sverjensky (2006) for the equilibrium constants for the formation of the tetra-species depending on the solid concentration was confirmed. Due to the lower oxide content used in this part of experiment, the surface complexation constants were converted for  $(> \text{SOH})_2(> \text{SO}^-)_2\text{Ca}^{2+}$  ( $\log K = -4.0$  for silica,  $\log K = -7.0$  for alumina) and for  $(> \text{SOH})_2(> \text{SO}^-)_2\text{CaOH}^+$  ( $\log K = 15.2$ ). It was found that to obtain the better fit of the electrokinetic data for silica in the presence of calcium

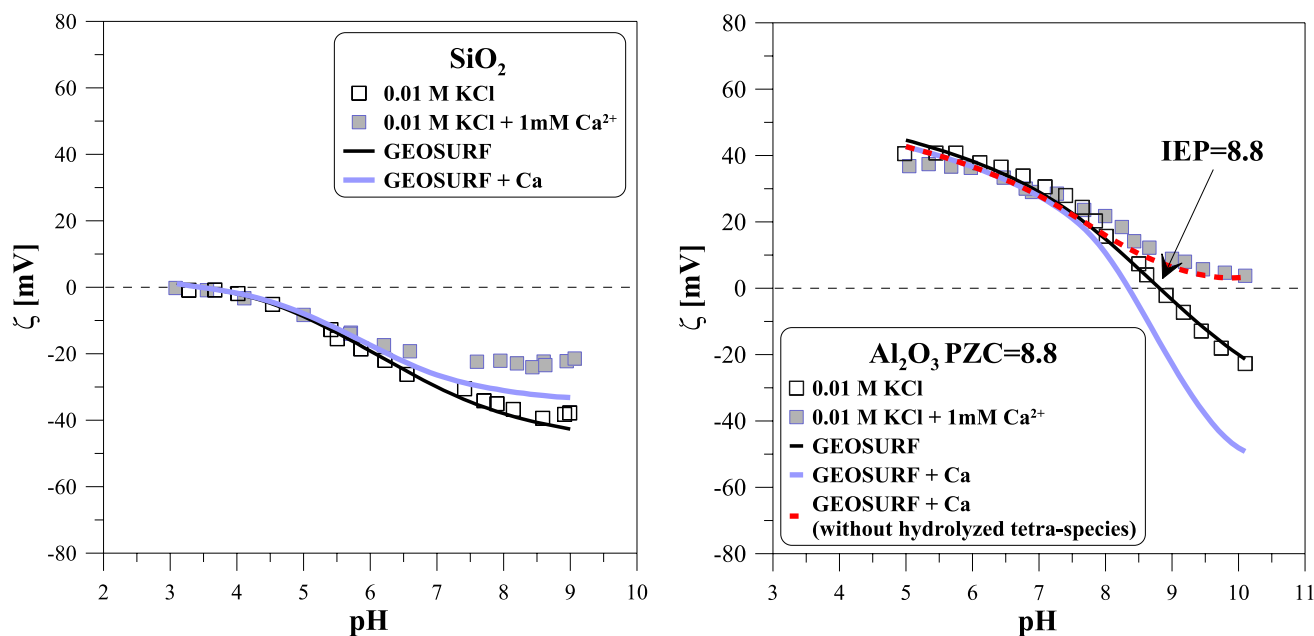


**Fig. 5** The pH dependence of  $\zeta$ -potential of  $\text{SiO}_2$  and  $\text{Al}_2\text{O}_3$  dispersions with  $\text{Ca}^{2+}$  (filled gray squares) and without (open gray squares) likened with the GEOSURF model fitting using the calcium speciation from Fig. 3 (solid line), and the modified speciation (dashed line)

excluding the tetra-species  $(> \text{SOH})_2(> \text{SO}^-)_2\text{Ca}(\text{OH})^+$  in the case of alumina. The oxide concentration was equal to  $1 \text{ g dm}^{-3}$  and the ionic strength to 0.01 M (Color figure online)



ions, there should be increased the value of  $\log K$  for the formation of the complex  $(>SOH)_2(>SO^-)_2Ca^{2+}$ . However, a worse fit of the other data would be obtained (not shown in this study). Such an increase of Ca complexation constant could be attributed to the higher calcium adsorption at a lower ionic strength according to the findings by Kosmulski (1994). For  $Al_2O_3$  the exclusion of the hydrolyzed tetra-species presented in Fig. 5 helped with fitting noticeably as it was in the case of maghemite in the previous paper (Szymanek et al. 2020). According to Sverjensky (2006) the adsorption mechanism may depend on ionic strength and solid concentration. It should be mentioned here that GEO-SURF applies Gouy–Chapman theory of DL, but diffuse layer charge is calculated taking into account all aqueous ion species, including  $Ca^{2+}$ .

## 4 Conclusions

We determined the proton surface charge, metal uptake and electrokinetic potential for  $Ca^{2+}$  adsorption on silica and alumina because the basic condition for obtaining reliable results applying surface complexation modeling is integration of many types of experimental data for the studied system. In our recent paper we made similar measurements for calcium adsorption on titanium dioxide and maghemite. The applied methodology led us to interesting observations. Firstly, the extent of calcium adsorption as a function of pH for silica and alumina is very similar and rather low. This means that electrostatic interactions between  $Ca^{2+}$  and the oxide surface are not a main driving force for adsorption because these two oxides are oppositely charged in the almost whole investigated pH range. Secondly, calcium ions have high affinity for  $TiO_2$ . As titanium dioxide has a very high dielectric constant compared with silica and alumina, this suggests that the changes in calcium ion solvation near the surface may have considerable influence on  $Ca^{2+}$  adsorption. In our research the modeling of the  $\zeta$ -potential data was the key of verifying the adsorbed metal species. The electrokinetic data excluded some  $Ca^{2+}$  surface complexes that appeared necessary to fit other experimental data. Probably, this discrepancy could be resolved by spectroscopic measurements (e.g. EXAFS). The stoichiometry of the calcium complexes on the oxide surface should be considered hypothetical, unless it has been verified by spectroscopic measurements.

Finally, we would like to mention some limitations of the TLM. This model does not take into account the change in the structure of interfacial water during ion adsorption. Variable surface charge and the accumulation of ions near the surface certainly affect the molecular properties of water. The 2-pK TLM also assumes that the entire charge of the adsorbed ion is located in one plane and not distributed

between the ions and the oxide surface as suggested by the CD-MUSIC model (Hiemstra and Van Riemsdijk 1996).

**Author contributions** Not applicable.

**Funding** Not applicable.

**Data availability** Not applicable.

**Code availability** Not applicable.

## Compliance with ethical standards

**Conflict of interest** All authors declare that they have no conflict of interest or financial ties to declare.

**Open Access** This article is licensed under a Creative Commons Attribution 4.0 International License, which permits use, sharing, adaptation, distribution and reproduction in any medium or format, as long as you give appropriate credit to the original author(s) and the source, provide a link to the Creative Commons licence, and indicate if changes were made. The images or other third party material in this article are included in the article's Creative Commons licence, unless indicated otherwise in a credit line to the material. If material is not included in the article's Creative Commons licence and your intended use is not permitted by statutory regulation or exceeds the permitted use, you will need to obtain permission directly from the copyright holder. To view a copy of this licence, visit <http://creativecommons.org/licenses/by/4.0/>.

## References

- Allen, N., Machesky, M., Wesolowski, D.J., Kabengi, N.: Calorimetric study of alkali and alkaline-earth cation adsorption and exchange at the quartz–solution interface. *J. Colloid Interface Sci.* **504**, 538–548 (2017)
- Atalay, S., Ma, Y., Qian, S.: Analytical model for charge properties of silica particles. *J. Colloid Interface Sci.* **425**, 128–130 (2014)
- Atesok, G., Somasundaran, P., Morgan, L.J.: Adsorption properties of  $Ca^{2+}$  on Na-kaolinite and its effect on flocculation using polyacrylamides. *Colloids Surf.* **32**, 127–138 (1988)
- Barbé, C., Bartlett, J., Kong, L., Finnie, K., Lin, Q.H., Larkin, M., Calleja, S., Bush, A., Calleja, G.: Silica particles: a novel drug-delivery system. *Adv. Mater.* **16**(21), 1959–1966 (2004)
- Brigante, M., Avena, M.: Biotemplated synthesis of mesoporous silica for doxycycline removal. Effect of pH, temperature, ionic strength and  $Ca^{2+}$  concentration on the adsorption behaviour. *Microporous Mesoporous Mater.* **225**, 534–542 (2016)
- Bui, T.-X., Choi, H.: Influence of ionic strength, anions, cations, and natural organic matter on the adsorption of pharmaceuticals to silica. *Chemosphere* **80**(7), 681–686 (2010)
- Chasserio, N., Guillemet-Fritsch, S., Lebey, T., Dagdag, S.: Ceramic substrates for high-temperature electronic integration. *J. Electron. Mater.* **38**(1), 164–174 (2009)
- Cheah, S., Brown, G.E., Jr., Parks, G.A.: XAFS study of Cu(II) sorption on amorphous silica and  $\gamma-Al_2O_3$ : effect of substrate and time on sorption complexes. *J. Colloid Interface Sci.* **208**, 110–128 (1998)

- Cherian, C., Kollannur, N.J., Bandipally, S., Arnepalli, D.N.: Calcium adsorption on clays: effects of mineralogy, pore fluid chemistry and temperature. *Appl. Clay Sci.* **160**, 282–289 (2018)
- Clapham, D.E.: Calcium signaling. *Cell* **131**(6), 1047–1058 (2007)
- Davis, J.A., James, R.O., Leckie, J.O.: Surface ionization and complexation at the oxide/water interface I. Computation of electrical double layer properties in simple electrolytes. *J. Colloid Interface Sci.* **63**(3), 480–499 (1978)
- Delgado, A.V., Gonzalez-Caballero, F., Hunter, R.J., Koopal, L.K., Lyklema, J.: Measurement and interpretation of electrokinetic phenomena (IUPAC Technical Report). *Pure Appl. Chem.* **77**(10), 1753–1805 (2005)
- Döpke, M.F., Lützenkirchen, J., Moulton, O.A., Siboulet, B., Dufrière, J.-F., Padding, J.T., Hartkamp, R.: Preferential adsorption in mixed electrolytes confined by charged amorphous silica. *J. Phys. Chem. C* **123**, 16711–16720 (2019)
- Eijssink, V.G.H., Matthews, B.W., Vriend, G.: The role of calcium ions in the stability and instability of a thermolysin-like protease. *Protein Sci.* **20**(8), 1346–1355 (2011)
- Eikenberg, J., Paul-Scherrer-Institut and Nationale Genossenschaft für die Lagerung radioaktiver Abfälle.: *On the Problem of Silica Solubility at High pH*. Paul Scherrer Institut, Villigen (1990)
- Fenter, P., Cheng, L., Rihs, S., Machesky, M., Bedyz, M.D., Sturchio, N.C.: Electrical double-layer structure at the rutile–water interface as observed *in situ* with small-period X-ray standing waves. *J. Colloid Interface Sci.* **225**, 154–165 (2000)
- Floch, P.L., Meixuanzi, S., Tang, J., Liu, J., Suo, Z.: Stretchable seal. *ACS Appl. Mater. Interfaces* **10**(32), 27333–27343 (2018)
- Frujtier-Pölloth, C.: The safety of nanostructured synthetic amorphous silica (SAS) as a food additive (E 551). *Arch. Toxicol.* **90**(12), 2885–2916 (2016)
- Hiemstra, T., Van Riemsdijk, W.H.: A surface structural approach to ion adsorption: the charge distribution (CD) model. *J. Colloid Interface Sci.* **179**(2), 488–508 (1996)
- Huang, C., Stumm, W.: Specific adsorption of cations on hydrous  $g\text{-Al}_2\text{O}_3$ . *J. Colloid Interface Sci.* **43**(2), 409–420 (1973)
- Izrael Živković, L.T., Živković, L.S., Jokić, B.J., Savić, A.B., Karadžić, I.M.: Adsorption of *Candida rugosa* lipase onto alumina: effect of surface charge. *J. Serb. Chem. Soc.* **80**(9), 1113–1125 (2015)
- Janusz, W., Patkowski, J., Chibowski, S.: Competitive adsorption of  $\text{Ca}^{2+}$  and  $\text{Zn(II)}$  ions at monodispersed  $\text{SiO}_2$ /electrolyte solution interface. *J. Colloid Interface Sci.* **266**, 259–268 (2003)
- Jia, Y., Zheng, Y., Lin, J., Zhang, G., Ma, X., Wang, X., Wang, S.: Surface sorption site and complexation structure of  $\text{Ca}^{2+}$  at the goethite–water interface: a molecular dynamics simulation and quantitative XANES analysis. *Bull. Environ. Contam. Toxicol.* **103**(1), 64–68 (2019)
- Kasprzyk-Hordern, B.: Chemistry of alumina, reactions in aqueous solution and its application in water treatment. *Adv. Colloid Interface Sci.* **110**, 19–48 (2004)
- Kendrick, N.C., Ratzlaff, R.W., Blaustein, M.P.: Arsenazo III as an indicator for ionized calcium in physiological salt solutions: its use for determination of the  $\text{CaATP}$  dissociation constant. *Anal. Biochem.* **83**(2), 433–450 (1977)
- Kosmulski, M.: Co-adsorption of mono- and multivalent ions on silica and alumina. *Ber. Bunsenges. phys. Chem.* **98**, 1062–1067 (1994)
- Kosmulski, M.: Compilation of PZC and IEP of sparingly soluble metal oxides and hydroxides from literature. *Adv. Colloid Interface Sci.* **152**, 14–25 (2009)
- Kosmulski, M., Hartikainen, J., Mączka, E., Janusz, W., Rosenholm, J.B.: Multiinstrument study of the electrophoretic mobility of fumed silica. *Anal. Chem.* **74**(1), 253–256 (2002)
- Lee, J., Mahendra, S., Alvarez, P.J.J.: Nanomaterials in the construction industry: a review of their applications and environmental health and safety considerations. *ACS Nano* **4**(7), 3580–3590 (2010)
- Lee, N., Sverjensky, D.A., Hazen, R.M.: Cooperative and competitive adsorption of amino acids with  $\text{Ca}^{2+}$  on rutile ( $\alpha\text{-TiO}_2$ ). *Environ. Sci. Technol.* **48**(16), 9358–9365 (2014)
- Lützenkirchen, J., Behra, P.: A new approach for modelling potential effects in cation adsorption onto binary (hydr)oxides. *J. Contam. Hydrol.* **26**, 257–268 (1997)
- Mayordomo, N., Foerstendorf, H., Lützenkirchen, J., Heim, K., Weiss, S., Alonso, U., Missana, T., Schmeide, K., Jordan, N.: Selenium(IV) sorption onto  $\gamma\text{-Al}_2\text{O}_3$ : a consistent description of the surface speciation by spectroscopy and thermodynamic modeling. *Environ. Sci. Technol.* **52**(2), 581–588 (2018)
- McCarthy, C.A., Ahern, R.J., Devine, K.J., Crean, A.M.: Role of drug adsorption onto the silica surface in drug release from mesoporous silica systems. *Mol. Pharm.* **15**, 141–149 (2018)
- McGrath, J.M., Spargo, J., Penn, C.J.: Soil fertility and plant nutrition. In: Alfen, N.V. (ed.) *Encyclopedia of Agriculture and Food Systems*, vol 5, pp. 166–184. Elsevier, San Diego (2014)
- Meng, X., Letterman, R.D.: Effect of component oxide interaction on the adsorption properties of mixed oxides. *Environ. Sci. Technol.* **27**(5), 970–975 (1993)
- Milonjić, S.K., Cerović, L.S., Cokesa, D.M., Zec, S.: The influence of cationic impurities in silica on its crystallization and point of zero charge. *J. Colloid Interface Sci.* **309**(1), 155–159 (2007)
- Pashley, M.R., Karaman, M.E.: *Applied Colloid and Surface Chemistry*. Wiley, Chichester (2004)
- Piasecki, W., Szymanek, K., Charnas, R.:  $\text{Fe}^{2+}$  adsorption on iron oxide: the importance of the redox potential of the adsorption system. *Adsorption* **25**(3), 613–619 (2019)
- Piontek, S.M., Tuladhar, A., Marshall, T., Borguet, E.: Monovalent and divalent cations at the  $\alpha\text{-Al}_2\text{O}_3$ (0001)/water interface: how cation identity affects interfacial ordering and vibrational dynamics. *J. Phys. Chem. C* **123**, 18315–18324 (2019)
- Prus, M., Szymanek, K., Mills, J., Lammers, L.N., Piasecki, W., Kędra-Królik, K., Zarzycki, P.: Electrophoretic and potentiometric signatures of multistage  $\text{CaCO}_3$  nucleation. *J. Colloid Interface Sci.* **544**, 249–256 (2019)
- Puigdomenech, I.: *MEDUSA: Make Equilibrium Diagrams Using Sophisticated Algorithms*. Royal Institute of Technology KTH, Stockholm (2001)
- Ragab, M.A.A., Korany, M.A., Ibrahim, H.Z., Abdel-Kawi, M.A., Sayed, A.E.A.A.A.: Adsorption behavior of some metal ions on nanoparticles used in pharmaceutical matrices: application to laboratory made drug formulation. *Bull. Fac. Pharm. Cairo Univ.* **55**, 155–162 (2017)
- Regalbutto, J.R., Navada, A., Shadid, S., Bricker, M.L., Chen, Q.: An experimental verification of the physical nature of Pt adsorption onto alumina. *J. Catal.* **184**(2), 335–348 (1999)
- Regi-Vallet, M., Balas, F.: Silica materials for medical applications. *Open Biomed. Eng. J.* **2**, 1–9 (2008)
- Ridley, M.K., Machesky, M.L., Wesolowski, D.J., Palmer, D.A.: Calcium adsorption at the rutile–water interface: a potentiometric study in  $\text{NaCl}$  media to 250 degrees C. *Geochim. Cosmochim. Acta* **63**(19–20), 3087–3096 (1999)
- Roach, T.L., Himmelblau, D.M.: The adsorption of calcium, strontium and thallium ions from molten salts by silica and alumina. *J. Inorg. Nucl. Chem.* **17**(3–4), 373–381 (1961)
- Ruchowski, L., Mączka, E., Kosmulski, M.: Dispersions of metal oxides in the presence of anionic surfactants. *Colloids Surf.* **3**(1), 3 (2018)
- Sahai, N.: Is silica really an anomalous oxide? Surface acidity and aqueous hydrolysis revisited. *Environ. Sci. Technol.* **36**, 445–452 (2002)
- Sahai, N., Sverjensky, D.A.: Evaluation of internally-consistent parameters for the triple-layer model by the systematic analysis of oxide surface titration data. *Geochim. Cosmochim. Acta* **61**, 2801–2826 (1997)

- Sahai, N., Sverjensky, D.A.: GEOSURF: a computer program for forward modeling of adsorption on mineral surfaces in aqueous solution. *Comput. Geosci.* **24**, 853–873 (1998)
- Sparks, D.L.: *Environmental Soil Chemistry*. Academic, Amsterdam (2003)
- Steiling, W., Almeida, J.F., Vandecasteele, H.A., Glipin, S., Kawamoto, T., O’Keeffe, L., Pappa, G., Rettinger, K., Rothe, H., Bowden, A.M.: Principles for the safety evaluation of cosmetic powders. *Toxicol. Lett.* **297**, 8–18 (2018)
- Stumm, W., Morgan, J.J.: *Aquatic Chemistry: Chemical Equilibria and Rates in Natural Waters*. Wiley, New York (1996)
- Sverjensky, D.A.: Prediction of surface charge on oxides in salt solutions: revisions for 1:1 ( $M^+L^-$ ) electrolytes. *Geochim. Cosmochim. Acta* **69**(2), 225–257 (2005)
- Sverjensky, D.A.: Prediction of the speciation of alkaline earths adsorbed on mineral surfaces in salt solutions. *Geochim. Cosmochim. Acta* **70**(10), 2427–2453 (2006)
- Szekeres, M., Tombácz, E.: Surface charge characterization of metal oxides by potentiometric acid–base titration, revisited theory and experiment. *Colloids Surf. A* **414**, 302–313 (2012)
- Szymanek, K., Charmas, R., Piasecki, W.: A study on the mechanism of  $Ca^{2+}$  adsorption on  $TiO_2$  and  $Fe_2O_3$  with the usage of calcium ion-selective electrode. *Chemosphere* **242**, 125162 (2020)
- Tadros, T.F., Lyklema, J.: The electrical double layer on silica in the presence of bivalent counter ions. *Electroanal. Chem. Interfacial Electrochem.* **22**, 1–7 (1969)
- Teaney, S., Pfaff, G., Nitta, K.: New effect pigments using innovative substrates. *Eur. Coat. J.* **4**, 90–96 (1999)
- Tombácz, E., Szekeres, M.: Interfacial acid–base reactions of aluminum oxide dispersed in aqueous electrolyte solutions. 1. Potentiometric study on the effect of impurity and dissolution of solid phase. *Langmuir* **17**, 1411–1419 (2001)
- Toner, C.V., Sparks, D.L.: Chemical relaxation and double layer model analysis of boron adsorption on alumina. *Soil Sci. Soc. Am. J.* **59**(2), 395–404 (1995)
- Villalobos, M., Leckie, J.O.: Surface complexation modeling and FTIR study of carbonate adsorption to goethite. *J. Colloid Interface Sci.* **235**, 15–32 (2001)
- Wan, B., Huang, R., Diaz, J.M., Tang, Y.: Polyphosphate adsorption and hydrolysis on aluminum oxides. *Environ Sci Technol* **53**(16), 9542–9552 (2019)
- Weng, L., Van Riemsdijk, W.H., Hiemstra, T.:  $Cu^{2+}$  and  $Ca^{2+}$  adsorption to goethite in the presence of fulvic acids. *Geochim. Cosmochim. Acta* **72**(24), 5857–5870 (2008)
- Westall, J.C.: FITEQL: A Program for the Determination of Chemical Equilibrium Constants from Experimental Data. Department of Chemistry, Oregon State University, Corvallis (1982)
- Wuddivira, M., Camps-Roach, G.: Effects of organic matter and calcium on soil structural stability. *Eur. J. Soil Sci.* **58**(3), 722–727 (2006)
- Yates, D.E., Levine, S., Healy, T.W.: Site-binding model of the electrical double layer at the oxide/water interface. *J. Chem. Soc. Faraday Trans. 1* **70**, 1807–1818 (1974)

**Publisher’s Note** Springer Nature remains neutral with regard to jurisdictional claims in published maps and institutional affiliations.

## Affiliations

Karolina Szymanek<sup>1</sup>  · Robert Charmas<sup>2</sup>  · Wojciech Piasecki<sup>3</sup> 

Robert Charmas  
rcharmas@pwsip.edu.pl

Wojciech Piasecki  
wojciech.piasecki@awf-bp.edu.pl

<sup>1</sup> Regional Research and Development Center, Józef Piłsudski University of Physical Education in Warsaw, Akademicka 2, 21-500 Biała Podlaska, Poland

<sup>2</sup> Faculty of Computer Science and Food Sciences, Łomża State University of Applied Sciences, Akademicka 14, 18-400 Łomża, Poland

<sup>3</sup> Faculty of Physical Education and Health, Józef Piłsudski University of Physical Education in Warsaw, Akademicka 2, 21-500 Biała Podlaska, Poland